

# Synthesis and Nearly Monochromatic Photoluminescence Properties of Conjugated Copolymers Containing Fluorene and Rare Earth Complexes

Q. D. Ling, E. T. Kang,\* and K. G. Neoh

Department of Chemical Engineering, National University of Singapore, Kent Ridge, Singapore 119260

Wei Huang\*

Institute of Advanced Materials and Technology, Fudan University, 220 Handan Road, Shanghai 200433, People's Republic of China

Received March 22, 2003; Revised Manuscript Received July 12, 2003

**ABSTRACT:** A series of novel conjugated copolymers containing 9,9-dihexylfluorene and europium complex-chelated benzoate units in the main chain had been synthesized through a three-step process, involving Suzuki coupling copolymerization, hydrolysis of benzoate units, and postchelation. The chemical structures of the copolymers were characterized by FT-IR,  $^1\text{H}$  NMR,  $^{13}\text{C}$  NMR, GPC, and ToF-SIMS. The copolymers exhibited relatively high glass transition temperatures after incorporation of the rare earth complexes. The photoluminescence (PL) properties of the copolymer complexes in solution and in film form were investigated. Intramolecular energy transfer from the fluorene groups to the europium complex occurred in diluted solutions of the copolymer. The efficiency of this process depended strongly on the structure of the ligands for the europium complex and the composition of the copolymers. The PL spectra of the copolymer complexes consisted of two emission bands, one in the 350–550 nm region and another at around 612 nm, corresponding to the  $\pi^* \rightarrow \pi$  transitions of the fluorene moieties and the f–f transitions of the europium ions, respectively. In the copolymer films cast from solutions, emission from the fluorene groups could be suppressed, and the absorbed excitation energy was transferred effectively to the europium complexes in the copolymer. Nearly monochromatic red emission (with a line width of about 4 nm) was detected under UV excitation at room temperature.

## Introduction

The first demonstration of efficient polymer light-emitting diodes (LEDs) in 1990<sup>1</sup> has spurred considerable interest in the application of conjugated semiconducting polymers for display technology.<sup>2</sup> Full color displays will require pure red, green, and blue emission. Obtaining monochromatic emission from conjugated polymers or small organic molecules is still difficult, since their emission spectra typically have a line width (full width at half-maximum, or fwhm) of 50–200 nm,<sup>3</sup> arising from the inhomogeneous broadening and the presence of vibronic progression. Moreover, in conjugated molecules, light is only generated from the singlet excitons, while the triplet excitons are lost in the nonradiative transitions. On the basis of spin statistics, only 25% of the excitons in conjugated molecules have the singlet character. Thus, the quantum efficiency of a conjugated polymer LED cannot exceed 25%.<sup>4</sup> The future development of polymer LEDs requires the synthesis of new materials that retain the inherent properties of conjugated polymer, such as the semiconductive properties and mechanical flexibility, and overcome the drawbacks of conjugated polymers, such as low efficiency and broad emission bands.

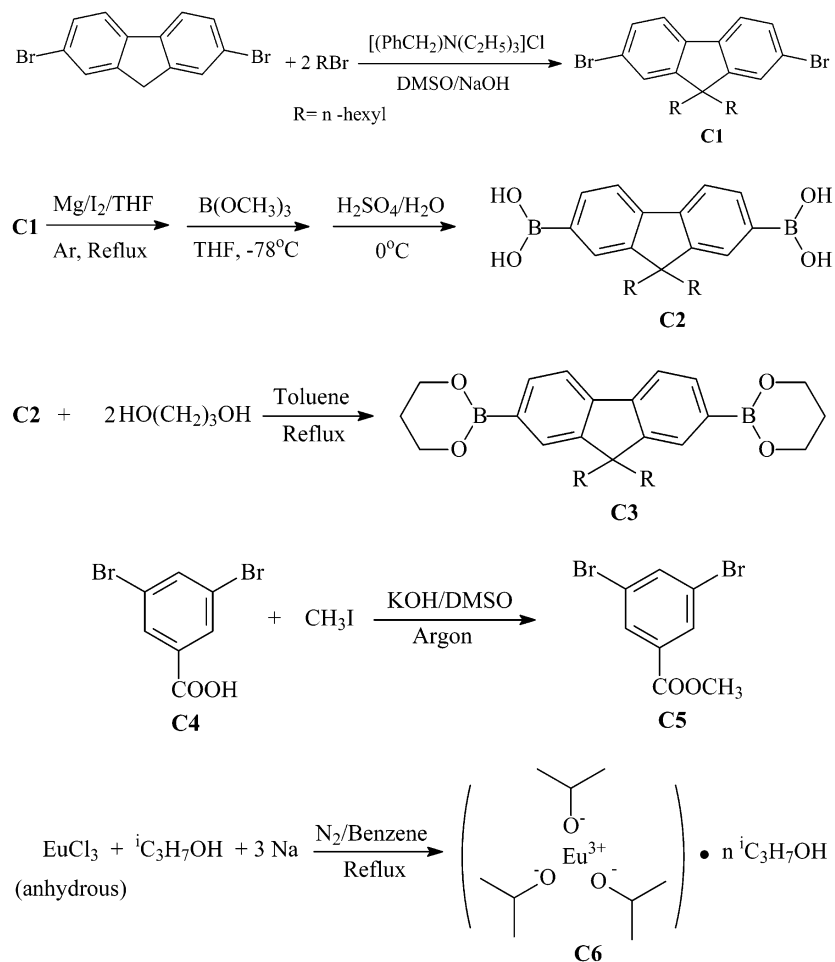
Rare earth compounds are excellent chromophores that exhibit intense fluorescence with a narrow spectral bandwidth (fwhm of 5–20 nm) and relatively long decay lifetime ( $10^{-2}$ – $10^{-6}$  s).<sup>5</sup> They are the most widely used materials in CRT displays and inorganic LEDs.<sup>6</sup> A great

deal of effort has also been devoted to the application of rare earth complexes in organic LEDs.<sup>7</sup> Pure red, green, blue, white, and infrared electroluminescence (EL) from the respective complexes of  $\text{Eu}^{3+}$ ,  $\text{Tb}^{3+}$ ,  $\text{Tm}^{3+}$ ,  $\text{Dy}^{3+}$ , and  $\text{Er}^{3+}$  have been reported.<sup>7,8</sup> However, many of the low-molecular-weight rare earth complexes undergo decomposition to some extent during film formation by vacuum deposition.<sup>9</sup> Decomposition of the rare earth complexes can be avoided in spin-coated films containing the rare earth complexes dispersed in polymer matrices.<sup>3,10</sup> A drawback of this technique is that nonuniform blending or dispersion of the dopants may result in phase separation and ionic aggregation.<sup>11</sup> The use of polymers with the lanthanide complexes covalently bonded in the main chain or as pendant groups will help to overcome the above-mentioned problems.

There are apparent advantages to incorporate the rare earth complexes into the conjugated polymers. First of all, since the emission from rare earth ions originates from transitions between the f levels that are well protected from environmental perturbations by the filled  $5s^2$  and  $5p^6$  orbitals, the resulting emission spectra are expected to be sharp and narrow. Second, the 25% limit on internal quantum efficiency of the conjugated polymers can be overcome, since not only the energy of the singlet, but also that of the triplet, can be transferred to lanthanide ions to generate the emission. Third, films can be cast directly from solutions of the rare earth complex-containing polymers, thereby facilitating the fabrication and improving the stability of the films. Finally, crystallization, phase separation, and ionic aggregation, which are detrimental to the performance of a device, can be avoided by binding the rare earth complex directly to the polymer backbone.

\* To whom all correspondence should be addressed: Fax +65-6779-1936 (E.T.K.), +86-21-6565-5123 (W.H.); e-mail cheket@nus.edu.sg (E.T.K.), wei-huang@fudan.edu.cn (W.H.).

Scheme 1. Synthetic Routes for the Monomers and Reagents



We have embarked on the design and synthesis of a series of conjugated copolymers containing europium complexes chelated to the main chains. The synthetic route, which involves Suzuki coupling copolymerization, hydrolysis, and postchelation, may be readily extended to the synthesis of other conjugated polymers containing other rare earth complexes, such as the  $\text{Tb}^{3+}$ ,  $\text{Nd}^{3+}$ ,  $\text{Tm}^{3+}$ , and  $\text{Er}^{3+}$  ion complexes. Such materials will permit the fabrication of pure red, green, and blue (RGB) polymer light-emitting devices as well as other photonic devices, such as lasers (based on Nd polymers) and amplifiers (based on Er polymers).

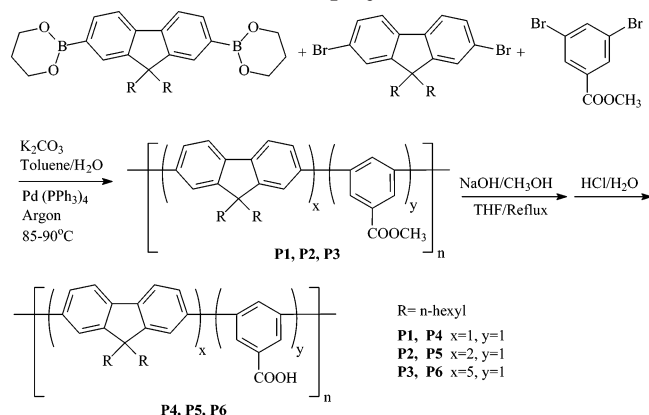
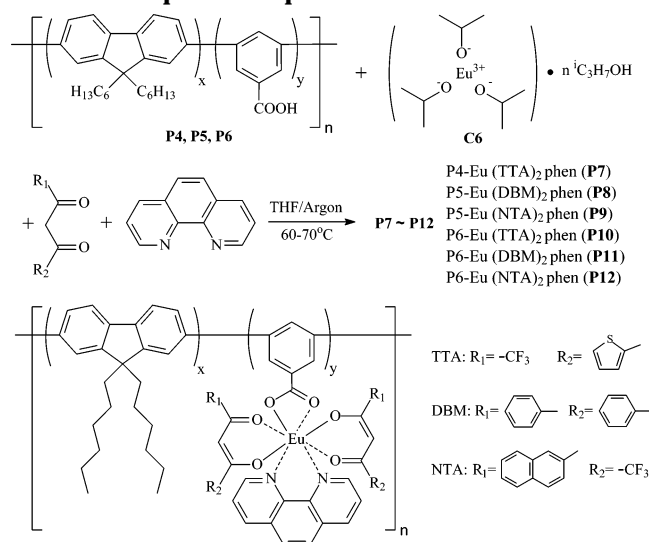
## Results and Discussion

**Design of the Conjugated Copolymers.** The emission efficiency of a rare earth complex depends strongly on the effective energy transfer from the polymer domain to the rare earth ions. This is a two-steps energy-transfer process involving<sup>3</sup> (a) Förster energy transfer from the conjugated blocks to the ligands and (b) Dexter energy transfer from the ligands to the excited states of the rare earth ions. To utilize both the Förster and Dexter energy transfer in the europium complex-containing polymer, a proper guest–host system must be selected. With a highly efficient emitting guest, the energy levels of the singlet and triplet excitons in the host must lie above the corresponding levels in the guest. Efficient energy transfer also requires the overlap of the emission spectrum in the host and the absorption spectrum in the guest. Since most of the rare earth complexes absorb in the region

of 200–400 nm, only those conjugated polymers with their emission bands falling in the ultraviolet or blue light region, such as polyfluorene, polycarbazole, poly(*p*-phenylene), poly(1,3,4-oxadiazole), and their derivatives,<sup>12,13</sup> may serve as the host. Fluorene and phenylene units are chosen to build the polymeric backbone since both of them are highly efficient blue emitting chromophores.<sup>14,15</sup> To improve the solubility of the copolymer in organic solvents, alkyl chains are introduced into the fluorene unit at the 9-position. It has been reported that polyfluorenes with substituted alkyl chains undergo changes in solubility and glass transition temperature, but not in the photoluminescence (PL) spectrum.<sup>16</sup>

To transfer energy from the ligands to the europium ions (the Dexter process), the triplet level of the ligands must be higher than the energy level of the first excited state ( $^5\text{D}_0$ ,  $17270 \text{ cm}^{-1}$ ) of the europium ions.<sup>17</sup> Moreover, for  $\text{Eu}(\text{III})$  ion, the energy levels of the first excited state ( $^5\text{D}_0$ ) and that of the second excited state ( $^5\text{D}_1$ ) are very close together. To reduce the nonradiative energy transfer between these two levels, the triplet level of the ligands and the first excited state of  $\text{Eu}(\text{III})$  ions must be as close to one another as possible. Some  $\beta$ -diketone ligands, such as thenoyltrifluoroacetone (TTA), dibenzoylmethane (DBM), and 1-(2-naphthoyl)-3,3,3-trifluoroacetone (NTA), meet the above criteria.<sup>18</sup>

**Synthesis of the Monomers and Copolymers.** The synthetic routes for the monomers are shown in Scheme 1. 2,7-Dibromo-9,9-dihexyl-9H-fluorene (**C1**) was synthesized in high yield (96%) by the reaction of 2,7-dibromofluorene with 1-bromohexane, catalyzed by

**Scheme 2. Synthetic Route and Molecular Structure of the Copolymers****Scheme 3. Synthetic Route and Molecular Structure of the Copolymers Containing Fluorene and Europium Complex in the Main Chain**

concentrated NaOH (aqueous, 50% w/w), and in the presence of a phase transfer catalyst, triethylbenzylammonium chloride. The substituted fluorene bromide reacted with magnesium in THF to form a bifunctional Grignard reagent, which was subsequently reacted with trimethyl borate at a low temperature ( $-78^\circ\text{C}$ ). The resulting fluorene boronate was hydrolyzed with 5%  $\text{H}_2\text{SO}_4$  to give the diboronic acid (**C2**) with a yield of 63%. The monomer, 2,7-bis(trimethylene boronate)-9,9-dihexyl-9H-fluorene (**C3**), was finally obtained (in 88% yield) by esterification of the diboronic acid with trimethylene glycol.<sup>19</sup> The other monomer, 3,5-dibromobenzoic acid (**C4**), was converted to the corresponding methyl benzoate (**C5**, yield 95%) by the highly efficient methylation of carboxylic acid with KOH/ $\text{CH}_3\text{I}$  in DMSO.<sup>20</sup>

The Suzuki coupling reaction<sup>21</sup> was applied to the synthesis of the copolymers of 2,7-bis(trimethylene boronate)-9,9-dihexyl-9H-fluorene and methyl 3,5-dibromobenzoate (**P1** to **P3**, Scheme 2). The advantages associated with this reaction include reactivity being less sensitive to steric hindrance, mild reaction conditions, less side reactions, and higher conversions.<sup>22</sup> Moreover, a well-defined alternating copolymer can be produced by this reaction. After copolymerization, the carboxylic groups were recovered by hydrolysis in methanol/THF and acidification.<sup>23</sup> The flossy solids so-

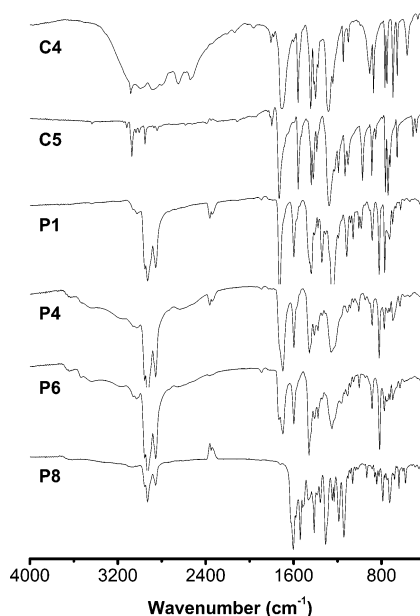


**Figure 1.** Comparison of infrared spectra of monomers and copolymers.

obtained (**P4** to **P6**) are soluble in THF but insoluble in toluene, acetone, chloroform, DMSO, and ethanol.

Rare earth complexes are commonly synthesized by dissolving the ligands in warm ethanol, neutralized to pH = 6 with a base, followed by the addition of the europium chloride solution.<sup>24</sup> This common procedure was applied to the preparation of the copolymer complexes in mixed solvents of THF and ethanol. It was found that the solubility of the copolymer became very poor in THF after neutralization with the aqueous NaOH. As a result, only a small portion of the carboxylic groups in the copolymer had successfully chelated the europium ions. To carry out the chelation of the europium ions in the absence of neutralization and to ensure the complete chelation of the carboxylic groups with the europium ions, a highly reactive europium salt, europium triisopropoxide (**C6**), was synthesized from anhydrous europium chloride (Scheme 1).<sup>25</sup> The salt is soluble in 2-propanol, benzene, and THF. The isopropoxy groups of the salt can be easily substituted by chelators, such as the carboxylic group and  $\beta$ -diketone, to form a europium complex in anhydrous organic solvents.<sup>26</sup> In this work, several copolymers containing the europium complexes in the main chain (**P7** to **P12**) were successfully prepared by this method (Scheme 3).

**Infrared Spectroscopy Results.** The representative FT-IR spectra of the copolymers are shown in Figure 1. For comparison, the FT-IR spectra of 3,5-dibromobenzoic acid (**C4**) and methyl 3,5-dibromobenzoate (**C5**) are also shown in Figure 1. Changes in the characteristic stretching absorption bands of the C=O and -OH groups are obvious in Figure 1. In the FT-IR spectrum of 3,5-dibromobenzoic acid, the C=O groups absorb at approximately  $1705\text{ cm}^{-1}$ . After esterification (**C5**), the C=O vibration has shifted to about  $1731\text{ cm}^{-1}$ , and the broad -OH stretching at around  $3100\text{ cm}^{-1}$  has disappeared. In the IR spectrum of the copolymer of methyl benzoate and 9,9-dihexylfluorene (**P1**), the C=O stretching ( $1728\text{ cm}^{-1}$ ) remains close to that of the corresponding monomer (**C5**). After hydrolysis, this characteristic C=O band of the copolymer (**P4**) has shifted back to  $1698\text{ cm}^{-1}$ , near that of the C=O band in 3,5-dibromobenzoic acid (**C4**). The typical broad absorption band of

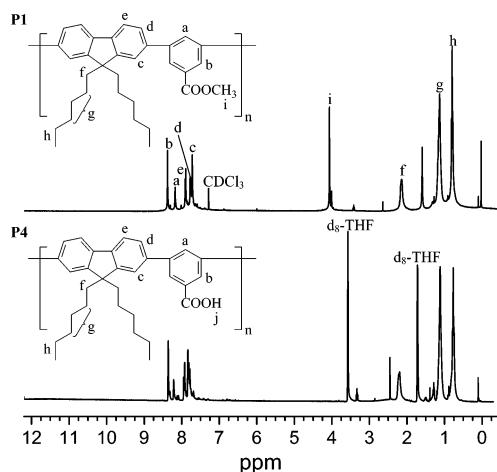


**Figure 2.** Comparison of  $^1\text{H}$  NMR spectra (300 MHz) of copolymers **P1** (in  $\text{CDCl}_3$ ) and **P4** (in  $d_8\text{-THF}$ ).

the  $-\text{OH}$  group has reappeared again. With the increase in fluorene to benzoate molar ratio in the copolymers ( $x/y = 1, 2,$  and  $5$ ; see Scheme 2), the absorption peak of the  $\text{C}=\text{O}$  groups in the copolymer becomes asymmetric after hydrolysis. A weak shoulder at about  $1733\text{ cm}^{-1}$  was also found in the spectrum of **P6**. This observation indicates that the ester groups of the copolymer were not hydrolyzed completely, probably due to the fact that hydrolysis of esters is a reversible reaction.

After incorporation of the europium complex, the FT-IR spectrum of the copolymer (**P8**) shows the absence of the  $\text{C}=\text{O}$  stretching vibration of the carboxylic group at  $1698\text{ cm}^{-1}$ , while the typical antisymmetric and symmetric stretching vibrations of the carboxylate group at about  $1579$  and  $1461\text{ cm}^{-1}$  have appeared.<sup>27</sup> The results suggest that the coordination bonds are formed between the  $\text{Eu}(\text{III})$  ion and the carboxylic group of the copolymer. Furthermore, the broad absorption band of the  $-\text{OH}$  group is almost undetectable, suggesting that most of the carboxylic groups of the copolymer are chelated to the europium ions. The  $\text{C}=\text{O}$  and  $\text{C}=\text{C}$  stretching vibrations of the  $\beta$ -diketone ligands coordinated with the complex are at about  $1623$  and  $1539\text{ cm}^{-1}$ , respectively. The ring vibration of the other ligand, 1,10-phenanthroline, is observed at  $1516\text{ cm}^{-1}$ , although the intensity is relatively weak. Other IR absorption bands at around  $1603$ ,  $1467$ , and  $1247\text{ cm}^{-1}$ , which are also observed in the spectra of the copolymers before chelation, are attributable to the aromatic ring stretching of the fluorene groups. In addition, two weak bands at  $641$  and  $581\text{ cm}^{-1}$ , associated with the  $\text{Eu}-\text{O}$  stretching vibrations,<sup>24</sup> are also observed. These FT-IR results further confirm the formation of the europium complex.

**$^1\text{H}$  NMR and  $^{13}\text{C}$  NMR.** Figure 2 shows the  $^1\text{H}$  NMR spectra of the copolymers before (**P1**) and after (**P4**) hydrolysis. The two main groups of peaks associated with chemical shifts at  $7.68$ – $8.36$  and  $0.74$ – $2.19\text{ ppm}$  can be attributed to the aromatic and the alkyl protons, respectively. The assignment of these peaks is given in Figure 2. The resonance of methyl protons on the ester group appears at a lower field of  $3.91\text{ ppm}$ . This chemical shift is not observed in the spectrum of the copolymer after hydrolysis, indicating that the hydrolysis of **P1** is almost complete. However, the resonance signal of the carboxylic proton is not observed in the  $10$ – $12\text{ ppm}$  region in the spectrum of the hydrolyzed

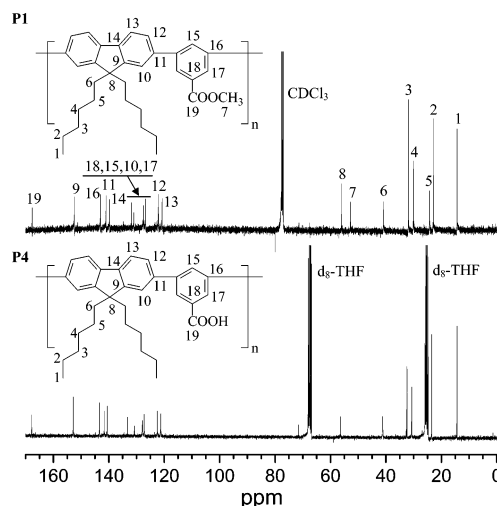


**Figure 3.** Comparison of  $^{13}\text{C}$  NMR spectra (75 MHz) of copolymers **P1** (in  $\text{CDCl}_3$ ) and **P4** (in  $d_8\text{-THF}$ ).

polymer. It is well-known that the  $^1\text{H}$  NMR signal of  $-\text{COOH}$  becomes weak and undetectable when the carboxylic group is in a complicated chemical environment due to the formation of H-bonds and association. The presence of a trace amount of water in the deuterated solvent may also affect the detection of  $-\text{COOH}$  group.

In the  $^{13}\text{C}$  NMR spectrum of the copolymer **P1** (shown in Figure 3), the chemical shifts for all the different carbon species are clearly shown in the 19 groups of peaks. The carboxyl carbon is bonded to two electron-withdrawing atoms (O), and the resonance is, therefore, expected at a very low field (at about  $167\text{ ppm}$ ). Because of the rigid five-member ring structure, the aromatic carbon of the fluorene group is susceptible to the ring current effect of the adjacent benzene rings. These carbon atoms are therefore deshielded and also appear at a lower field. Other chemical shifts can be assigned reasonably to the aromatic and aliphatic carbon atoms.<sup>16</sup> The  $^{13}\text{C}$  NMR spectra of the copolymer before and after hydrolysis are similar, although they have been measured in different solvents. However, the chemical shift of the methyl carbon in the ester group at about  $52.8\text{ ppm}$  has disappeared in the spectrum of the copolymer after hydrolysis (**P4**). This result indicates again that the hydrolysis of the copolymer **P1** is almost complete.

The  $^1\text{H}$  NMR and  $^{13}\text{C}$  NMR spectra of the copolymer complex **P8** are shown in Figure 4. Because of the paramagnetic nature of the  $\text{Eu}(\text{III})$  ion, the  $^1\text{H}$  NMR peaks of the protons around the atoms, such as O and N, may shift substantially to a lower field.<sup>28</sup> Actually, europium- $\beta$ -diketone complexes have been widely used as "shift reagents" in NMR measurements.<sup>29</sup> As shown in Figure 4, the  $^1\text{H}$  NMR spectrum of  $\text{P5-Eu}(\text{DBM})_2\text{phen}$  (**P8**) is very complicated. There are four weak chemical shifts in the low magnetic field region ( $10.89$ ,  $10.49$ ,  $9.90$ , and  $8.89\text{ ppm}$ ). These four peaks are roughly attributed to the protons near the coordinated atoms in the ligands, viz., dibenzoylmethane (DBM), benzoate and 1,10-phenanthroline (phen). It is difficult to assign the peaks individually. However, the aromatic and aliphatic protons of the fluorene group are not affected since they are further away from the coordination center. Their chemical shifts are similar to those of the copolymer before chelation. A well-resolved  $^{13}\text{C}$  NMR spectrum of the copolymer complex **P8** is shown in Figure 4. In the regions of chemical shift for the



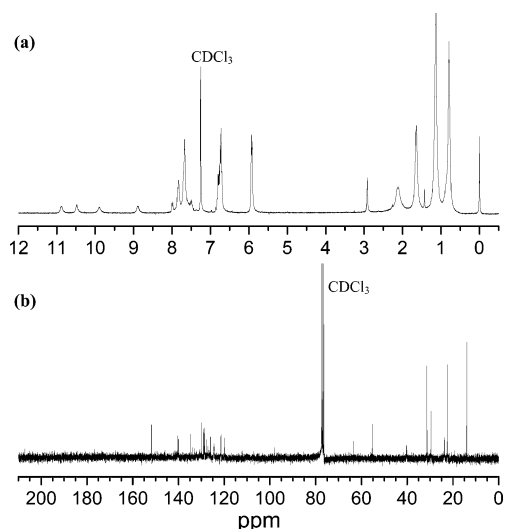


**Figure 4.** (a)  $^1\text{H}$  NMR (300 MHz) and (b)  $^{13}\text{C}$  NMR (75 MHz) of the copolymer complex **P8** in  $\text{CDCl}_3$ .

**Table 1. Molecular Weight and Polydispersity Index (PDI) of the Copolymers**

polymer	$\bar{M}_n (\times 10^4)$	$\bar{M}_w (\times 10^4)$	PDI	$P (\%)^a$
<b>P1</b>	0.82	1.38	1.69	
<b>P2</b>	1.37	3.02	2.20	
<b>P3</b>	3.18	10.1	3.18	
<b>P4</b>	0.96	1.35	1.43	
<b>P5</b>	1.65	3.34	2.03	
<b>P6</b>	3.90	9.90	2.54	
<b>P4-Eu(TTA)<sub>2</sub>phen (P7)</b>	1.63	3.16	1.94	62.6
<b>P5-Eu(DBM)<sub>2</sub>phen (P8)</b>	3.11	9.80	3.15	94.4
<b>P5-Eu(NTA)<sub>2</sub>phen (P9)</b>	2.83	8.32	2.94	82.0
<b>P6-Eu(TTA)<sub>2</sub>phen (P10)</b>	4.18	11.3	2.70	74.8
<b>P6-Eu(DBM)<sub>2</sub>phen (P11)</b>	4.11	10.6	2.58	73.4
<b>P6-Eu(NTA)<sub>2</sub>phen (P12)</b>	4.06	9.78	2.41	70.2

<sup>a</sup>  $P(\%)$  is the degree of chelation of the  $-\text{COOH}$  groups. Assume 100% hydrolysis, the degree of chelation is calculated as shown in the following example:  $P(\%) = [(\bar{M}_n \text{ of P7})/(\bar{M}_n \text{ of P4})] \div [(\bar{M} \text{ of repeat unit of P7})/(\bar{M} \text{ of repeat unit of P4})] \times 100\% = [(1.63 \times 10^4)/(0.96 \times 10^4)] \div [(1227.27/452.7) \times 100\%] = 62.6\%$ .

aromatic (119.8–151.7 ppm) and aliphatic (13.91–55.24 ppm) carbon atoms, the spectrum is similar to that of the copolymer before chelation, except that new peaks have appeared in the aromatic region due to the contribution of the carbon atoms of the ligands. This result indicates that the effect of europium complex to the carbon atoms, which are not bonded directly to the coordinated oxygen atoms, is not obvious.

**Molecular Mass.** The molecular weights and polydispersity indexes (PDI) of the copolymers were measured by gel permeation chromatography (GPC) using THF as the eluent and polystyrene standards as the references. The results are shown in Table 1. With the increase in monomer ratio of fluorene to benzoate ( $x/y = 1, 2$ , and  $5$ ; see Scheme 2), the molecular weight of the copolymer (from **P1** to **P3** or **P4** to **P6**) increases unambiguously. This phenomenon can be explained by the solubility of the resulting copolymers. Since the fluorene monomer contains two long alkyl side chains, the increase in fluorene content can improve the solubility of the resulting copolymer during condensation, thus allowing the polymerization to proceed without phase separation. Comparison of the molecular size data of the copolymers (**P1**, **P2**, and **P3**) to those of their hydrolyzed counterparts (**P4**, **P5**, and **P6**) reveals that the molecular weight ( $\bar{M}_n$ ) increases and polydispersity decreases after hydrolysis. These phenomena suggest

that the copolymers have been further purified after the hydrolysis and acidification reactions, although the phenomena can probably also be attributed, in part, to the inadequacy of the standards used in the GPC measurements. The most significant feature observed in Table 1 is that the molecular weight of the copolymer containing the europium complex (**P7**, **P8**, and **P10**) is much higher than that of corresponding copolymer prior to the coordination of the europium complex. This result provides further confirmation to the successful formation of the polymer complex.

The degree of chelation ( $P\%$ ) of the  $-\text{COOH}$  groups is calculated and listed in Table 1. The values suggest that only about half of the carboxylic groups in copolymer **P7** coordinate with the europium ions. Because of the steric hindrance of the complex and the high density of the carboxylic groups in the copolymer, the neighboring carboxylic groups may have been prevented from chelating the europium ions. The degree of chelation in **P10** is also only about 75%. It is likely that some ester groups, which cannot chelate the europium ions, exist in **P6** due to the incomplete hydrolysis of **P3** (see the FT-IR results of **P6**). It appears that **P5** is more suitable for coordination complex formation than **P4** and **P6**. The  $P\%$  of  $-\text{COOH}$  groups in **P8** is as high as 94.4%. Taking into account of the incomplete hydrolysis, there is probably no free carboxylic group remaining in **P8**. It is well-known that the existence of the carboxylic group will quench the excitons when the material is used as the emitting layer.<sup>30</sup> The highly active europium triisopropoxide ensure the complete coordination of the carboxylic groups with the  $\text{Eu(III)}$  ions. Such materials provide the possibility of high quantum efficiencies when LED devices are fabricated utilizing these polymers as the emitting layer.

Mass fragments of the copolymer complexes are revealed by the time-of-flight secondary ion mass spectrometry (ToF-SIMS). ToF-SIMS is useful for the determination of the molecular structures of polymers, such as the repeat units, side chains, end groups, and functional groups.<sup>31</sup> Figure 5 shows the positive ion ToF-SIMS spectra of the copolymer containing the europium complex (**P8**). The assignments of the main positive ion fragments are shown in the mass spectra. The main europium complex fragment containing the carboxylate is found at 835 ( $M/z$ ), indicating that the europium complex has been successfully coordinated to the carboxylic groups of the copolymer. Other fragments containing the europium complex are also found in the high mass region ( $M/z = 550\text{--}780$ ). In the mid-mass region ( $M/z = 200\text{--}500$ ), fragments of the polymers backbone (fluorene and phenylene) and the ligands (DBM and phen) are found. The europium ion appears in the spectrum at  $M/z$  around 152, as expected. The spectrum in the mass range 0–120 shows the presence of species associated with the alkyl side chain. Thus, the ToF-SIMS results reveal the structure of the copolymer containing the europium complex.

**Thermal Properties.** The thermal properties of the copolymers under nitrogen or air have been investigated using differential scanning calorimetry (DSC) and thermogravimetric analysis (TGA). The results are shown in Table 2 and Figure 6, respectively. Copolymer complex **P7** shows weight loss commencing at about 125  $^\circ\text{C}$ . This polymer contains residual carboxylic groups (see Table 1), which fail to coordinate with the europium ions due to steric hindrance. The residual  $-\text{COOH}$

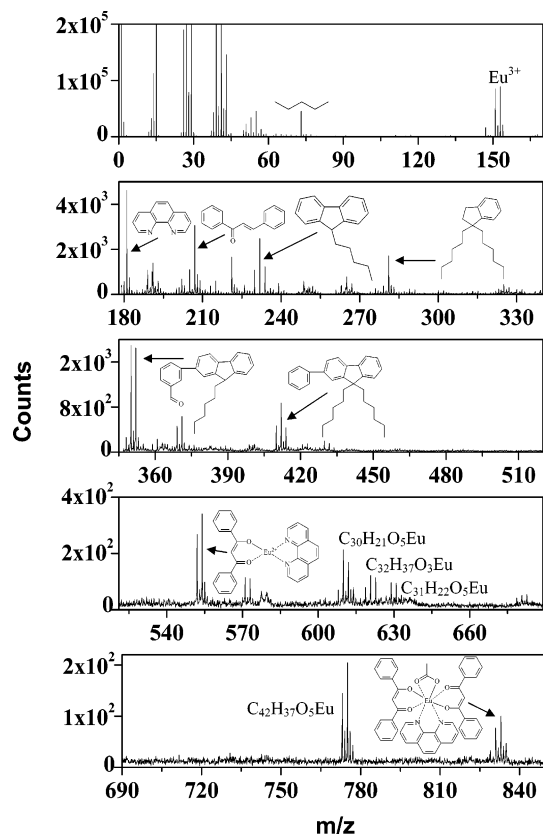


**Figure 5.** Positive ion ToF-SIMS spectra of **P8** film spin-cast from THF solution on ITO glass.

**Table 2. Relative Efficiency of Energy Transfer and Thermal Property of the Copolymers**

polymer	Eu% (w/w) <sup>a</sup>	<i>T<sub>g</sub></i> (°C) (midpoint)	<i>T<sub>d</sub></i> (°C) <sup>d</sup> (onset)	<i>I<sub>Eu</sub></i> / <i>I<sub>F</sub></i> <sup>c</sup>	
				solution	film
<b>P3</b>		115.8	388.6		
<b>P4</b> -Eu(TTA) <sub>2</sub> phen ( <b>P7</b> )	9.43	192.3 <sup>b</sup>	125.6	0.59	
<b>P5</b> -Eu(DBM) <sub>2</sub> phen ( <b>P8</b> )	9.11	127.3	315.6	0.21	98.9
<b>P5</b> -Eu(NTA) <sub>2</sub> phen ( <b>P9</b> )	8.77	126.7	317.8		0.08
<b>P6</b> -Eu(TTA) <sub>2</sub> phen ( <b>P10</b> )	3.61	124.8	316.4	0.07	4.04
<b>P6</b> -Eu(DBM) <sub>2</sub> phen ( <b>P11</b> )	3.24				40.7
<b>P6</b> -Eu(NTA) <sub>2</sub> phen ( <b>P12</b> )	2.93				0.04

<sup>a</sup> Eu% (w/w): the content of europium ion in the copolymer. The Eu content is lower than that calculated from the degree of chelation because of incomplete hydrolysis. <sup>b</sup> Note that weight loss happened before this temperature. <sup>c</sup> The relative efficiency of energy transfer is defined as the fluorescence intensity ratio: *I<sub>Eu</sub>*/*I<sub>F</sub>*, where *I<sub>Eu</sub>* is the maximum intensity of the main emission peak of europium complex at around 612 nm and *I<sub>F</sub>* is the maximum intensity of the main emission peak of fluorene groups in the range of 412–422 nm. <sup>d</sup> Temperature for the onset of thermal decomposition.

groups tend to adsorb moisture. The adsorbed solvent is given off when the polymer is heated to above 100 °C in the air. The major thermal degradation occurred at about 312 °C. No weight loss was observed in the low-temperature region for the other two copolymer complexes (**P8** and **P10**), suggesting that all the free carboxylic groups have coordinated with the europium ions. These two copolymer complexes exhibit only a major weight loss commencing at about 315 °C. The glass transition temperature (*T<sub>g</sub>*) of the copolymers was measured by DSC at a heating rate of 10 °C/min and a nitrogen flow rate of 70 cm<sup>3</sup>/min. The *T<sub>g</sub>* of the copolymer with 5:1 molar ratio of fluorene: phenylene (**P3**) is about 115 °C (Table 2). In comparison with **P3**, the *T<sub>g</sub>*

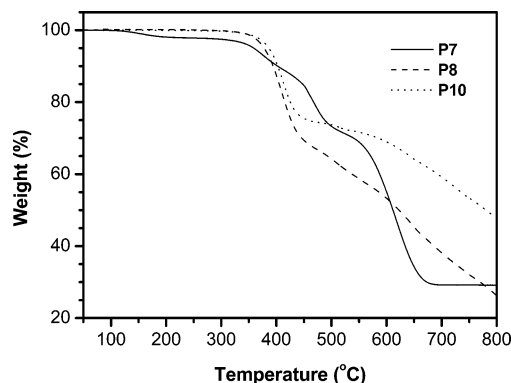


**Figure 6.** Thermogravimetric analysis of copolymers **P7** (solid curve), **P8** (dashed curve), and **P10** (dotted curve) carried out in air.

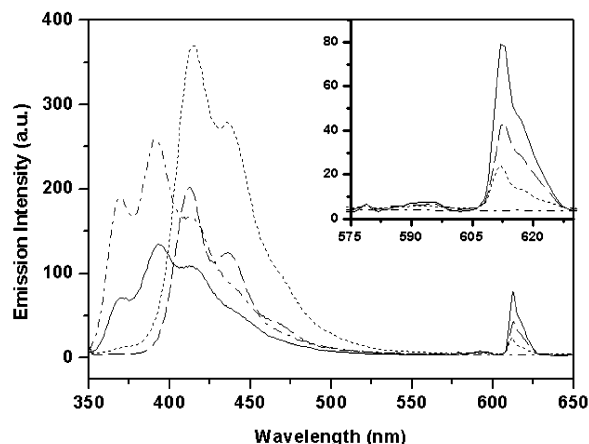


**Figure 7.** Comparison of the PL spectra of the copolymers containing europium complex in dilute solution ( $1.0 \times 10^{-5}$  mol (repeat unit)/L, THF as solvent,  $\lambda_{\text{ex}} = 350$  nm): **P7** (solid curve), **P8** (dashed curve), **P10** (dotted curve), and **P1** doped with Eu(DBM)<sub>3</sub>phen (dash-dotted curve).

of the copolymer containing the europium complex (**P10**) has increased by  $\sim 10$  °C. These *T<sub>g</sub>* values are much higher than those of other polyfluorenes (*T<sub>g</sub>*  $\sim 50$ – $100$  °C).<sup>32</sup> The relatively high *T<sub>g</sub>*'s of the present copolymer complexes are advantageous to applications as emissive materials in light-emitting diodes.<sup>33</sup>

**Photoluminescence in Solution.** To investigate the energy transfer between the fluorene group (donor) and the europium complex (acceptor), the optical properties of the copolymers were studied first in diluted solution ( $10^{-5}$  mol/L) at room temperature. Figure 7 shows the photoluminescence (PL) spectra of three copolymer complexes (**P7**, **P8**, and **P10**) and a copolymer (**P1**) doped with the europium complex. Every spectrum (except for the spectrum of the doped copolymer) consists of two groups of emission peaks. The first group is in the range 350–550 nm. This broad emission band is associated with the  $\pi^* \rightarrow \pi$  transitions of the fluorene moieties of the copolymers. In the cases of **P8** and **P10**, the emission band has a sharp emission peak at 413 nm and a shoulder at about 436 nm (fwhm of about 50 nm). The relatively sharp emission peak arises from the radiative decay of singlet excitons.<sup>34</sup> As shown in Figure 7, the PL spectrum of **P7** is quite different from those of **P8** and **P10**. The main emission peak of fluorene is apparently blue-shifted to 393 nm. In addition to the shoulder at about 414 nm, a new shoulder appears at about 370 nm. The latter is attributable to the emission

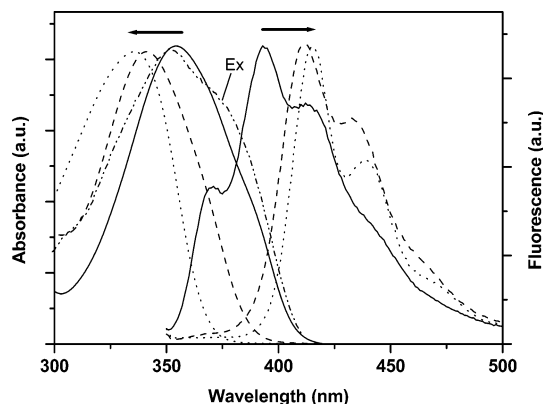


**Figure 8.** Absorption spectra of Eu(DBM)<sub>3</sub>phen (solid curve), Eu(TTA)<sub>3</sub>phen (dashed curve), and Eu(NTA)<sub>3</sub>phen (dotted curve); excitation and emission spectra ( $\lambda_{\text{ex}} = 350$  nm) of **P1** (solid curve), **P2** (dashed curve), and **P3** (dotted curve) in THF. Note that the intensities were arbitrarily chosen in order to optimally fit the spectra.

from a monofluorene unit. These phenomena arise from the difference in effective conjugation length of this copolymer. Since **P7** is an alternating copolymer of fluorene and *m*-phenylene, the *m*-phenylene group develops a poor coplanarity with the fluorene unit and reduces the effective conjugated length of the copolymer. **P8** and **P10** are random copolymers (Scheme 2), in which the neighboring fluorene groups are not separated in the backbone. As a result, the effective conjugation length of the copolymers is extended.

The other emission group consists of three narrow peaks (enlarged in the inset of Figure 7), which originate from the transitions between the 4f states of the europium ion in the copolymers. The three PL peaks centered at 578, 593, and 613 nm are attributable to the  $^5\text{D}_0 \rightarrow ^7\text{F}_0$ ,  $^5\text{D}_0 \rightarrow ^7\text{F}_1$ , and  $^5\text{D}_0 \rightarrow ^7\text{F}_2$  transitions, respectively.<sup>24</sup> Note that emission from the europium complex is not detected in the case of **P1** doped by Eu(DBM)<sub>3</sub>phen, having the same europium content as that of **P7**. Because the absorption band of Eu(DBM)<sub>3</sub>phen is buried under the excitation spectrum of **P1** (Figure 8), the excitation energy was entirely absorbed by copolymer **P1**. Moreover, the europium complex (acceptor) fails to accept the energy generated by the radiative decay from fluorene group (donor) of **P1**. In such a diluted solution, the europium complex and the fluorene group are separated from each other by a distance more than the critical distance for Förster energy transfer. However, in the cases of **P7**, **P8**, and **P10**, the europium complex is directly bonded to the main chain of the copolymer. Thus, the distance between the donor and the acceptor is fixed and is not influenced by the diluted solution environment. Intramolecular Förster energy transfer does happen between the fluorene group and the europium complex in the copolymer, as the emissions from the europium complexes are detected in diluted solutions. More recently, a series of conjugated polyfluorenes with the europium complex in the side chain have been synthesized in our group.<sup>35</sup> However, the Förster energy transfer only occurs in the solid state. The same phenomenon has often been reported in conjugated polymer system doped with a small europium complex.<sup>3,36</sup> It seems more reasonable to attribute this process to intermolecular energy transfer rather than to the intramolecular process, since the long alkyl side chain may have physically separated the donor from the acceptor.

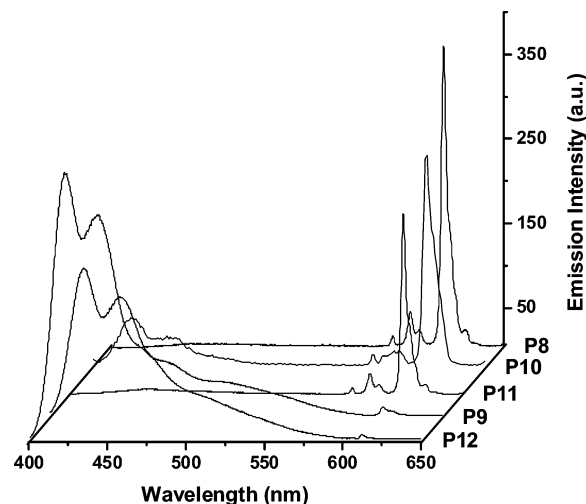


**Figure 9.** Photoluminescence spectra of the polymer films formed by spin-coating from THF solutions on ITO glass substrates.

The relative energy-transfer efficiency in the copolymer containing the europium complex is determined from the ratio of the maximum emission intensities of the two chromophores (Table 2). As shown in Table 2 and Figure 7, **P7** has the highest energy-transfer efficiency in solution compared to the other copolymers of similar europium content. For the same polymer backbone, the copolymer complexes with DBM as the  $\beta$ -diketone ligand usually have a higher efficiency (Table 2) compared to those with other  $\beta$ -diketone ligands (TTA and NTA). This phenomenon is due to different degrees of overlap between the emission spectrum of the fluorene and the absorption spectrum of the europium complex in the copolymers. The spectral overlap between the fluorene emission and europium complex absorption in diluted solution is shown in Figure 8. Because of the blue shift of the emission spectrum, **P1** has a larger degree of spectral overlap than the other two polymers (**P2** and **P3**), with the different europium complexes. The absorption peaks of the europium complexes with different  $\beta$ -diketone ligands are red-shifted according to  $\text{NTA} < \text{TTA} < \text{DBM}$ . Their spectral overlap with a particular polymer increases as the above sequence. When the europium complexes are incorporated into the copolymers, the energy-transfer efficiency of the resulting copolymer complexes will be dependent on the extent of spectral overlap.

**Photoluminescence in the Solid State.** Figure 9 shows the PL spectra of the copolymer films formed by spin-casting from THF solutions on ITO glass substrates. Because of the formation of excimers, the emission spectrum of the fluorene groups is red-shifted by about 10 nm and undergoes broadening. The formation of excimers is a common phenomenon in conjugated molecules in solid state.<sup>37</sup> The effective conjugation length is extended in the excimers, leading to the red shift of the emission spectrum. However, the emission peak of the europium complex remains at about 612 nm.

Comparison of the fluorescence spectrum of **P8** film with the corresponding solution spectrum reveals distinct differences (see Figures 7 and 9). Blue light is the dominant emission in solution. However, it has disappeared almost completely in the solid state. This difference indicates that the efficiency of energy transfer in the solid state is much higher than that in solution. The phenomenon arises from the fact that the distance



between the donor and the acceptor is very small in the solid state. In addition to the intramolecular energy transfer, intermolecular energy transfer also takes place in the solid state.

Nearly monochromatic red emission spectra, with a fwhm of about 4 nm, are obtained from the films of **P8** and **P11** (Figure 9). These two copolymers contain the same  $\beta$ -diketone ligand (DBM) in the europium complex. The absorption spectrum of this Eu complex has the largest degree of spectral overlap with the emission spectrum of the donor copolymer. Thus, the energy-transfer efficiencies in **P8** and **P11** are much higher than those in the other copolymers. These two copolymer complexes are excellent candidates for fabricating pure red light-emitting devices, since they have both the semiconductive properties of conjugated polymers and the pure red emission characteristics of europium complexes. There is also a sharp red emission peak at 613 nm (fwhm = 8 nm) in the PL spectrum of the film from **P10**. However, the blue emission from the fluorene groups is not completely suppressed in this film.

## Conclusions

A series of novel conjugated copolymers containing fluorene and rare earth complexes in the main chain were synthesized. The synthetic route to these polymers involved three steps. First of all, a series of copolymers of 2,7-bis(trimethylene boronate)-9,9-dihexyl-9H-fluorene and methyl 3,5-dibromobenzoate were synthesized through a palladium-catalyzed Suzuki coupling reaction. The copolymers were then hydrolyzed to provide the active carboxylic ligands in the main chains. Finally, the polymeric ligand, together with the  $\beta$ -diketone ligands and 1,10-phenanthroline, chelated the highly reactive europium triisopropoxide to form the desirable copolymer complexes. FT-IR, NMR, GPC, and ToF-SIMS results revealed the successful formation of the designed copolymer complexes. Unlike the small molecular rare earth complexes, these copolymer complexes were soluble in THF and could be cast into transparent films with good mechanical flexibility. The aggregation of the europium ions in the copolymer films was completely avoided. The copolymer complexes exhibited much higher glass transition temperatures ( $T_g$ ) than the other polyfluorene derivatives. The copolymer complexes were capable of both blue and red emissions under UV excitation. When the copolymer complexes were dissolved in solution, blue emission was the dominant mode. However, the blue emission was significantly reduced in the solid state. For copolymer complexes **P8** and **P11**, the blue emission was completely suppressed and nearly monochromatic red emission (with a fwhm of about 4 nm) was observed. This phenomenon was attributed to the effective Förster energy transfer from the fluorene group to the europium complex in these copolymer complexes. Efficient intramolecular energy transfer was possible since the two chromophores were connected in the same polymer backbone. These novel photoluminescent properties may enable them to be used as pure red-emitting materials for full color RGB displays.

## Experimental Section

**Measurements.**  $^1\text{H}$  and  $^{13}\text{C}$  NMR spectra were collected on a Bruker ACF 300 spectrometer with  $d$ -chloroform or  $d_8$ -THF as the solvent and tetramethylsilane as the internal standard. FT-IR spectra were recorded on a Bio-Rad FTS 165

spectrometer by dispersing the samples in KBr pellets. UV-vis and fluorescence spectra were obtained on a Shimadzu UV-NIR 3100 spectrophotometer and on a Shimadzu RF 5301PC luminescence spectrophotometer, respectively. Thermogravimetric analysis (TGA) was conducted on a TA Instruments TGA 2050 thermogravimetric analyzer at a heating rate of 20 °C/min and under an air flow rate of 75 mL/min. Differential scanning calorimetry (DSC) measurements were carried out on the Mettler Toledo DSC 822° system under  $\text{N}_2$  and at a heating rate of 10 °C/min. Europium contents were measured by titration with EDTA standard solution. Concentrated  $\text{HClO}_4$  and  $\text{HNO}_3$  were used to decompose the polymer samples before titration. ToF-SIMS analysis was carried out on an ION-TOF SIMS IV instrument (ION-TOF, GmbH, Germany). The polymer films were spin-cast from the THF solution onto ITO glass substrates. In the analysis, the primary ion beam (10 keV  $\text{Ar}^+$ ) with a spot size of about 50  $\mu\text{m}$  was rastered over an area of  $500 \times 500 \mu\text{m}^2$  while keeping the total dose under  $10^{13}$  ions/ $\text{cm}^2$ . The pressure in the analysis chamber was maintained at  $1.0 \times 10^{-9}$  Torr or lower during measurement. To reduce the charging effect, an electron flood gun was used for the charge neutralization. Gel permeation chromatography (GPC) analysis was conducted on a HP 1100 HPLC system equipped with the HP 1047A RI detector and the Agilent 79911GP-MXC columns, using standard polystyrene samples as the molecular weight references and THF as the eluent.

**Materials.** Europium oxide with high purity (99.99%) was supplied by Shanghai Yuelong Nonferrous Metal Ltd Co., China. Other starting materials and reagents were purchased from Aldrich Chemical Co. Tetrahydrofuran (THF) was refluxed over sodium in the presence of benzophenone until a persistent blue color appeared and then distilled. Other GR or HPLC grade solvents were purchased from Merck-Schuchardt Chemical Co. and were used without further purification (unless otherwise stated). The catalyst, tetrakis(triphenylphosphine)palladium ( $\text{Pd}(\text{PPh}_3)_4$ ), was freshly prepared according to the method reported in the literature.<sup>38</sup>

**General Procedures for the Preparation of Poly[2,7-(9,9-dihexylfluorene)-co-5-(methoxycarbonyl)phenylene-1,3-diyl].** Under an argon atmosphere, monomer **C3** and monomer **C5** (or plus **C2**) were mixed together with 1.0–1.5% (mol) of  $\text{Pd}(\text{PPh}_3)_4$  in a small flask. Degassed aqueous solution of potassium carbonate (2.0 M) and toluene (3:5, volume ratio) were added to the reactor. The mixture was stirred vigorously at 80–90 °C for 72 h under an argon atmosphere. The resulting solution was added dropwise into stirring methanol to precipitate the polymer. The fibrous solid was collected by filtration and washed with methanol and water. The material was washed continuously with acetone for 2 days in a Soxhlet extractor to remove the oligomers and catalyst residues. The product was dried under reduced pressure overnight. **P1** was a pale yellow solid (yield 85.4%). **P2** was a gray flossy solid (yield 88.1%). **P3** was a gray flossy solid (yield 85.6%).

**General Procedures for the Preparation of Poly[2,7-(9,9-dihexylfluorene)-co-5-carboxyphenylene-1,3-diyl].** Under the protection of argon, poly[2,7-(9,9-dihexylfluorene)-co-5-(methoxycarbonyl)phenylene-1,3-diyl] (**P1**, **P2**, or **P3**) was dissolved in THF and refluxed with a solution of sodium hydroxide (5–10 wt %) in methanol (THF/MeOH = 1:1, in volume). With the hydrolysis in progress, the solution became opaque, and a substantial amount of insoluble solid appeared after 24 h. The reaction was allowed to proceed for another 24 h. The reaction mixture was poured into 100 mL of distilled water with vigorous stirring to form a milky solution. After acidified with diluted hydrochloric acid (0.5 M), the resulting white material was isolated by filtration and washed thoroughly with doubly distilled water. The crude product was dissolved in THF and then reprecipitated in an excess volume of methanol under vigorous stirring. This procedure was repeated 2–3 times. The polymer was dried in a vacuum oven at 50 °C for 24 h. **P4** was a light brown solid (yield 96.6%). **P5** was a light yellow flossy solid (yield 90.6%). **P6** was an off-white solid (yield 84.0%).



**General Procedures for the Preparation of Copolymers Containing Europium Complex (P7–P12).** All the glassware was prebaked at 110 °C, cooled under vacuum, and purged with nitrogen. 0.294 mmol of europium triisopropoxide (**C6**) in the mixed solvent of benzene and 2-propanol (1:1, volume ratio) was injected into a flask and then diluted with dried THF (3 mL). The solution was warmed to 60 °C in an oil bath. A solution of 0.294 mmol of poly[2,7-(9,9-dihexylfluorene)-co-5-carboxyphenylene-1,3-diyl] (**P4**, **P5**, or **P6**) in dried THF was added dropwise into the flask by means of a syringe. The reaction took place immediately, and a white viscous solid appeared. The reaction mixture was kept under stirring and refluxing for half an hour under an argon atmosphere. A calculated amount of  $\beta$ -diketone ligand was dissolved in 5 mL of THF and added dropwise into the reaction mixture over a period of 15 min. As the chelation progressed, the viscous solid redissolved to form a clear solution. After 5 h, the last ligand, 1,10-phenanthroline (anhydrous), in 2 mL of THF was added. The reaction was continued for another hour. The resulting solution was concentrated and dropped into water to precipitate the polymer. The crude product was washed thoroughly with hot ethanol to remove the residue ligands and small molecular complexes. The polymer was dried in a vacuum oven at 50 °C for 24 h. Yield: 65–87%.

**Acknowledgment.** The authors thank the Agency for Science, Technology and Research (A\*STAR) of Singapore for financial support under the Project Grant MCE/00/002.

**Supporting Information Available:** Comprehensive data/results from  $^1\text{H}$  and  $^{13}\text{C}$  NMR, FT-IR, and mass spectroscopic analyses for compounds **C1**, **C2**, **C3**, and **C5** and for copolymers **P1** through **P6**; melting point and elemental analysis data for the four compounds. This material is available free of charge via the Internet at <http://pubs.acs.org>.

## References and Notes

- Burroughes, J. H.; Bradley, D. D. C.; Brown, A. R.; Marks, R. N.; Mackay, K.; Friend, R. H.; Burns, P. L.; Holmes, A. B. *Nature (London)* **1990**, *347*, 539.
- (a) Rees, I. D.; Robinson, K. L.; Holmes, A. B.; Towns, C. R.; O'Dell, R. *MRS Bull.* **2002**, *27*, 451. (b) Tonzola, C. J.; Alam, M. M.; Jenekhe, S. A. *Adv. Mater.* **2002**, *14*, 1086. (c) Xia, C. J.; Advincula, R. C. *Macromolecules* **2001**, *34*, 5854. (d) Friend, R. H.; Gymer, R. W.; Holmes, A. B.; Burroughes, J. H.; Marks, R. N.; Taliani, C.; Bradley, D. D. C.; DosSantos, D. A.; Bredas, J. L.; Logdlund, M.; Salaneck, W. R. *Nature (London)* **1999**, *397*, 121. (e) Ho, P. K. H.; Thomas, D. S.; Friend, R. H.; Tessler, N. *Science* **1999**, *285*, 233.
- McGehee, M. D.; Bergstedt, T.; Zhang, C.; Saab, A. P.; O'Regan, M. B.; Bazan, G. C.; Srdanov, V. I.; Heeger, A. J. *Adv. Mater.* **1999**, *11*, 1349.
- Friend, R.; Burroughes, J.; Shimoda, T. *Phys. World* **1999**, *12*, 35.
- Sinha, A. P. B. In *Spectroscopy in Inorganic Chemistry*; Rao, C. N. R., Ferraro, J. R., Eds.; Academic: New York, 1971; Vol. 2.
- Jüstel, T.; Nikol, H.; Ronda, C. *Angew. Chem., Int. Ed.* **1998**, *37*, 3084.
- Kido, J.; Okamoto, Y. *Chem. Rev.* **2002**, *102*, 2357 and references therein.
- (a) Sun, R. G.; Wang, Y. Z.; Zheng, Q. B.; Zhang, H. J.; Epstein, A. J. *J. Appl. Phys.* **2000**, *87*, 7589. (b) Hong, Z. R.; Liang, C. J.; Li, R. G.; Li, W. L.; Zhao, D.; Fan, D.; Wang, D. Y.; Chu, B.; Zang, F. X.; Hong, L. S.; Lee, S. T. *Adv. Mater.* **2001**, *13*, 1241. (c) Kido, J.; Hayase, H.; Hongawa, K.; Nagai, K.; Okuyama, K. *Appl. Phys. Lett.* **1994**, *65*, 2124.
- Uekawa, M.; Miyamoto, Y.; Ikeda, H.; Kaifu, K.; Nakaya, T. *Bull. Chem. Soc. Jpn.* **1998**, *71*, 2253.
- (a) Nigel, A. H. M.; Salata, O. V.; Christou, V. *Synth. Met.* **2002**, *126*, 7. (b) Peng, J. B.; Takada, N.; Minami, N. *Thin Solid Films* **2002**, *405*, 224. (c) Liang, C. J.; Li, W. L.; Yu, J. Q.; Liu, X. Y.; Li, D.; Zhao, Y.; Peng, J. B. *Chin. J. Lumin.* **1996**, *17*, 382.
- Segura, J. L. *Acta Polym.* **1998**, *49*, 319 and references therein.
- Brizius, G.; Kroth, S.; Bunz, U. H. F. *Macromolecules* **2002**, *35*, 5317.
- Kim, D. Y.; Cho, H. N.; Kim, C. Y. *Prog. Polym. Sci.* **2000**, *25*, 1089.
- Pogantsch, A.; Wenzl, F. P.; List, E. J. W.; Leising, G.; Grimsdale, A. C.; Mullen, K. *Adv. Mater.* **2002**, *14*, 1061.
- Arker, A. M.; Gurel, E. E.; Zheng, M.; Lahti, P. M.; Karasz, F. E. *Macromolecules* **2001**, *34*, 5897.
- Fukuda, M.; Sawada, K.; Yoshino, K. *J. Polym. Sci., Part A: Polym. Chem.* **1991**, *31*, 2465.
- Dieke, G. H.; Crosswhite, H. M. *Appl. Opt.* **1963**, *2*, 675.
- Dawson, W. R.; Kropp, J. L.; Windsor, M. W. *J. Chem. Phys.* **1966**, *45*, 2410.
- Yu, W. L.; Pei, J.; Cao, Y.; Huang, W.; Heeger, A. J. *Chem. Commun.* **1999**, *18*, 1837.
- Avila-Zárraga, J. G.; Martínez, R. *Synth. Commun.* **2001**, *32*, 2177.
- Miyaura, N.; Suzuki, A. *Chem. Rev.* **1995**, *95*, 2457.
- Schlüter, A. D.; Wegner, G. *Acta Polym.* **1993**, *44*, 59.
- Kaeriyama, K.; Mehta, M. A.; Masuda, H. *Synth. Met.* **1995**, *69*, 507.
- Moeller, T. *Gmelin Handbook of Inorganic Chemistry*; Springer-Verlag: New York, 1981; Vol. 39(D3), pp 65–232.
- Sinha, R. P. N. *Sci. Culture* **1960**, *25*, 494.
- (a) Wang, L. H.; Wang, W.; Zhang, W. G.; Kang, E. T.; Huang, W. *Chem. Mater.* **2000**, *12*, 2212. (b) Ling, Q. D.; Yang, M. J.; Wu, Z. F.; Zhang, X. M.; Wang, L. H.; Zhang, W. G. *Polymer* **2001**, *42*, 4605.
- Li, L. M.; Zeng, G. B.; Zhuang, W. D. *Acta Chim. Sin. (Engl. Ed.)* **1988**, *46*, 9.
- Dong, D. W.; Jiang, B. Z. *Mater. Chem. Phys.* **2002**, *78*, 501.
- Reuben, J.; Elgavish, G. A. In *Handbook on the Physics and Chemistry of Rare Earths*; Gschneidner, K. A., Eyring, L., Jr., Eds.; North-Holland: Amsterdam, 1979; Vol. 4, Part II, pp 483–514.
- Yan, M.; Rothberg, L. J.; Papadimitrakopoulos, F.; Galvin, M. E.; Miller, T. M. *Phys. Rev. Lett.* **1994**, *73*, 744.
- Muilenberg, G. E. *Handbook of X-ray Photoelectron Spectroscopy*; Perkin-Elmer: Eden Prairie, MN, 1978; p 38.
- Liu, B. Ph.D. Dissertation, National University of Singapore, Singapore, 2001.
- Tokito, S.; Tanaka, H.; Noda, K.; Okada, A.; Taga, Y. *Appl. Phys. Lett.* **1997**, *70*, 1929.
- Cho, H. N.; Kim, D. Y.; Kim, J. K.; Kim, C. Y. *Synth. Met.* **1997**, *91*, 293.
- Liu, X. L. Master Thesis, National University of Singapore, Singapore, 2002.
- Zhong, G. L.; Kim, K. K.; Jin, J. I. *Synth. Met.* **2002**, *129*, 193.
- Prieto, I.; Teetsov, J.; Fox, M. A.; Bout, D. A. V.; Bard, A. J. *J. Phys. Chem. A* **2001**, *105*, 520.
- Coulson, D. R. *Inorganic Syntheses*; McGraw-Hill: New York, 1972; Vol. XIII, p 121.

MA034362D